Supplement of

Satellite-based, top-down approach for the adjustment of aerosol precursor emissions over East Asia: TROPOMI product, and the Geostationary Environment Monitoring Spectrometer (GEMS) data fusion product and its proxy

Jincheol Park and Jia Jung et al.

Correspondence to: Yunsoo Choi (ychoi6@uh.edu)

Table S1. Model configurations.

WRF 3.8	
Domain	East Asia on 27 km × 27 km grids
Microphysics	Morrison double-moment scheme (Morrison *et al*., 2009)
Longwave and shortwave radiation	Rapid Radiative Transfer Model for GCMs (RRTMG) (Clough *et al*., 2005; Iacono *et al*., 2008)
Land surface	Pleim-Xiu land surface model (Xiu and Pleim, 2001)
Surface layer	Pleim-Xiu surface layer (Pleim, 2006)
Planetary boundary layer	ACM2 planetary boundary layer model (Pleim 2007a, 2007b)
Cumulus parameterization	Kain-Fritch (new Eta) scheme (Kain, 2004)
Four-Dimensional Data Assimilation	FDDA option for grid-nudging (Jeon *et al*., 2015)
Initial and boundary conditions for meteorology	1° × 1° National Centers for Environmental Prediction (NCEP) FNL (final) operational model global analysis data
CMAQ 5.2 and CMAQ DDM-3D 5.2	
Horizontal advection	YAMO
Vertical advection	WRF omega formula
Horizontal diffusion	Multiscale
Vertical diffusion	ACM2 vertical diffusion scheme (Pleim 2007a, 2007b)
Chemical mechanism and aerosol processing module	SAPRC-07 and AERO6 (Carter, 2010; Simon, 2015)
Dry deposition model	M3Dry (Pleim *et al*., 2001)

Table S2. The list of the primary PM species included the KORUS-AQ emission inventory, and the corresponding pollutants simulated in CMAQ version 5.2 and measured at the Korean supersites.

KORUS-AQ emissions species	Corresponding CMAQ species	Corresponding Korean supersite species	Description
PSO4	ASO4J	$PM_{2.5}SO_4$	Fine mode sulfate
PNO3	ANO3J	$PM_{2.5}NO_3$	Fine mode nitrate
PCL	ACLJ	$PM_{2.5}Cl$	Fine mode particulate chloride
PNH4	ANH4J	$PM_{2.5}NH_4$	Fine particulate ammonium
PNA	ANAJ	$PM_{2.5}Na$	Fine mode sodium
PCA	ACAJ	$PM_{2.5}Ca$	Fine mode calcium
PMG	AMGJ	$PM_{2.5}Mg$	Fine mode magnesium
PK	AKJ	$PM_{2.5}K$	Fine mode potassium
POC	APOCI, APOCJ	$PM_{2.5}OC$	Fine mode primary organic carbon
PNCOM	APNCOMI, APNCOMJ	-	Fine mode primary non-carbon organic matter
PEC	AECI, AECJ	$PM_{2.5}EC$	Fine mode elemental carbon
PFE	AFEJ	$PM_{2.5}Fe$	Fine mode iron
PAL	AALJ	-	Fine mode aluminum
PSI	ASIJ	-	Fine mode silicon
PTI	ATIJ	$PM_{2.5}Ti$	Fine mode titanium
PMN	AMNJ	$PM_{2.5}Mn$	Fine mode manganese
PH2O	AH2OJ	-	Fine mode particulate water
PMOTHR	AOTHRJ	$PM_{2.5}V$, $PM_{2.5}Cr$, $PM_{2.5}Ni$, $PM_{2.5}Cu$, $PM_{2.5}Zn$, $PM_{2.5}As$, $PM_{2.5}Se$, $PM_{2.5}Br$, $PM_{2.5}Pb$	Remaining unspeciated (undefined) fine mode primary PM
PMC	ACORS	-	Coarse mode primary PM

Table S3. Summary statistics between the WRF-simulated hourly meteorological fields (2 m air temperatures (°C), and 10 m wind U and V components (m/s)) and ground-based in-situ measurements in Korea during the study periods 2019 (132 sites) and 2022 (95 sites). R: Pearson's correlation coefficient, IOA: index of agreement, RMSE: root mean square error, MB: mean bias.

	2019			2022		
	Air temperature	Wind U	Wind V	Air temperature	Wind U	Wind V
R	0.98	0.64	0.52	0.95	0.65	0.48
IOA	0.99	0.74	0.69	0.96	0.75	0.66
RMSE	2.34	1.68	1.55	2.81	1.56	1.41
MB	-1.00	0.16	-0.21	-1.56	0.49	0.02

Table S4. Seasonal and yearly mean NO_x emissions (tons/day) before (a priori) and after (a posteriori) the NO_x emissions adjustment over the modeling domain during the study period 2019. MAM: March, April, and May, JJA: June, July, and August, SON: September, October, and November, DJF: December, January, and February.

	MAM	JJA	SON	DJF	Yearly
A priori	2.21	2.28	2.17	2.17	2.21
A posteriori	4.98	6.25	4.72	3.73	4.92
Difference (post - prior) (%)	125.08	174.16	117.68	71.64	122.79

Table S5. Summary statistics of the CMAQ-simulated daily mean surface NO_2 concentrations (ppb) before (a priori) and after (a posteriori) the NO_x emission adjustment and ground-based in-situ measurements (346 sites in Korea and 235 sites in the NCP region) during the study period 2019. R: Pearson's correlation coefficient; NMB (%): normalized mean bias.

		Korea		NCP	
		A priori	A posteriori	A priori	A posteriori
MAM	R	0.66	0.72	0.75	0.75
	NMB	-24.20	-5.66	-13.90	12.34
JJA	R	0.45	0.63	0.54	0.52
	NMB	15.63	1.83	5.25	22.32
SON	R	0.72	0.82	0.50	0.55
	NMB	-2.06	21.66	-11.43	15.24
DJF	R	0.75	0.76	0.55	0.59
	NMB	-23.54	13.45	-1.05	33.75
Yearly	R	0.71	0.84	0.76	0.78

	NMB	-12.11	8.51	-6.00	21.70

Table S6. Seasonal and yearly mean primary PM emissions (g/s) before (a priori) and after (a posteriori) the primary PM emissions adjustments (the emissions adjustments using the AHI AOD and GOCI-AHI fused AOD) over the modeling domain during the study period 2019. The primary PM emissions here indicate the total amount of all primary PM species listed in Table S2.

		MAM	JJA	SON	DJF	Yearly
Emissions adjusted using AHI AOD	A priori	13.45	11.90	12.35	15.19	13.22
	A posteriori	21.19	21.61	19.55	31.79	23.53
	Difference (post - prior) (%)	57.54	81.62	58.27	109.30	76.68
Emissions adjusted using GOCI-AHI AOD	A priori	13.45	11.90	12.35	15.19	13.22
	A posteriori	28.28	28.91	23.16	33.08	28.36
	Difference (post - prior) (%)	110.30	142.96	87.54	117.73	114.63

Table S7. Monthly and 3-month mean NO_x emissions (tons/day) before (a priori) and after (a posteriori) the NO_x emissions adjustment over the modeling domain during the study period 2022.

	MAR	APR	MAY	3-month
A priori	0.83	0.82	0.82	0.82
A posteriori	0.80	0.71	0.76	0.76
Difference (post - prior) (%)	-2.83	-13.40	-7.33	-7.84

Table S8. Monthly and 3-month mean primary PM emissions (g/s) before (a priori) and after (a posteriori) the primary PM emissions adjustments (using GEMS-AMI-GOCI-2 fused AOD) over the modeling domain during the study period 2022. The primary PM emissions here indicate the total amount of all primary PM species listed in Table S2.

	MAR	APR	MAY	3-month
A priori	14.61	12.80	12.61	13.34
A posteriori	10.35	13.67	12.38	12.14
Difference (post - prior) (%)	-29.17	6.86	-1.81	-9.03

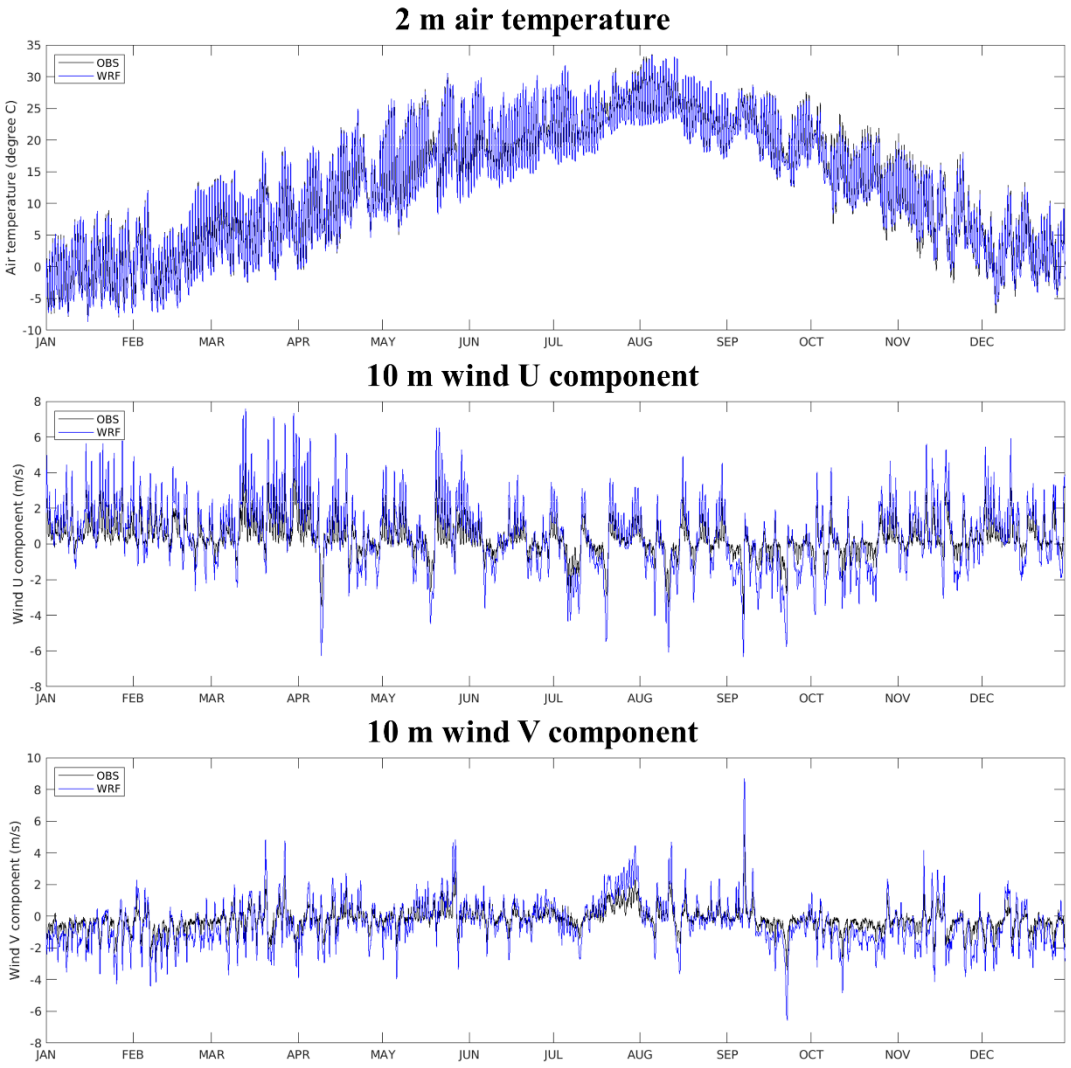

Figure S1. Time-series comparisons between WRF-simulated hourly meteorological fields (2 m air temperatures (°C), and 10 m wind U and V components (m/s)) and ground-based in-situ measurements in Korea during the study period 2019 (132 sites). OBS: ground-based in-situ measurements, WRF: WRF-simulated meteorological fields.

45

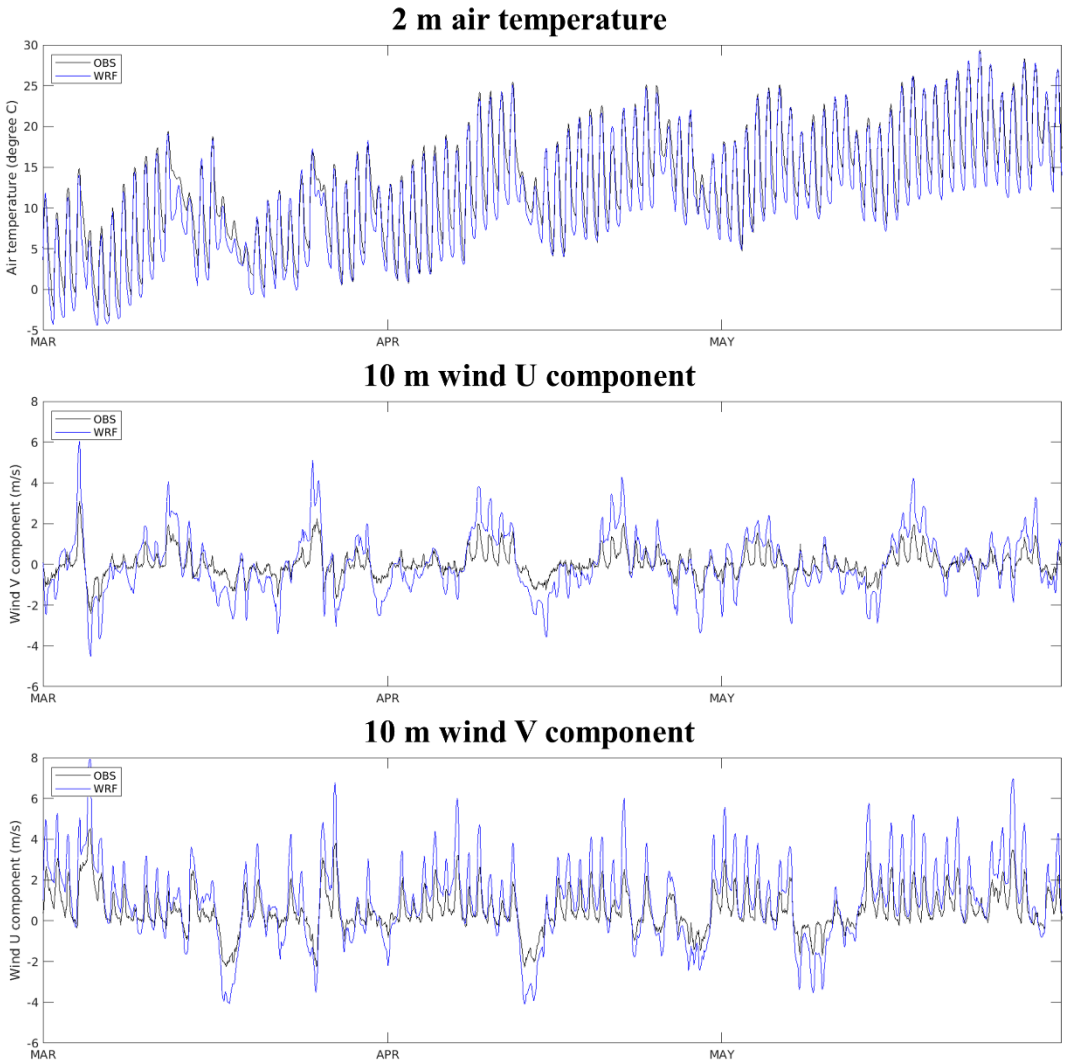

Figure S2. Time-series comparisons between WRF-simulated hourly meteorological fields (2 m air temperatures (°C), and 10 m wind U and V components (m/s)) and ground-based in-situ measurements in Korea during the study period 2022 (95 sites). OBS: ground-based in-situ measurements, WRF: WRF-simulated meteorological fields.

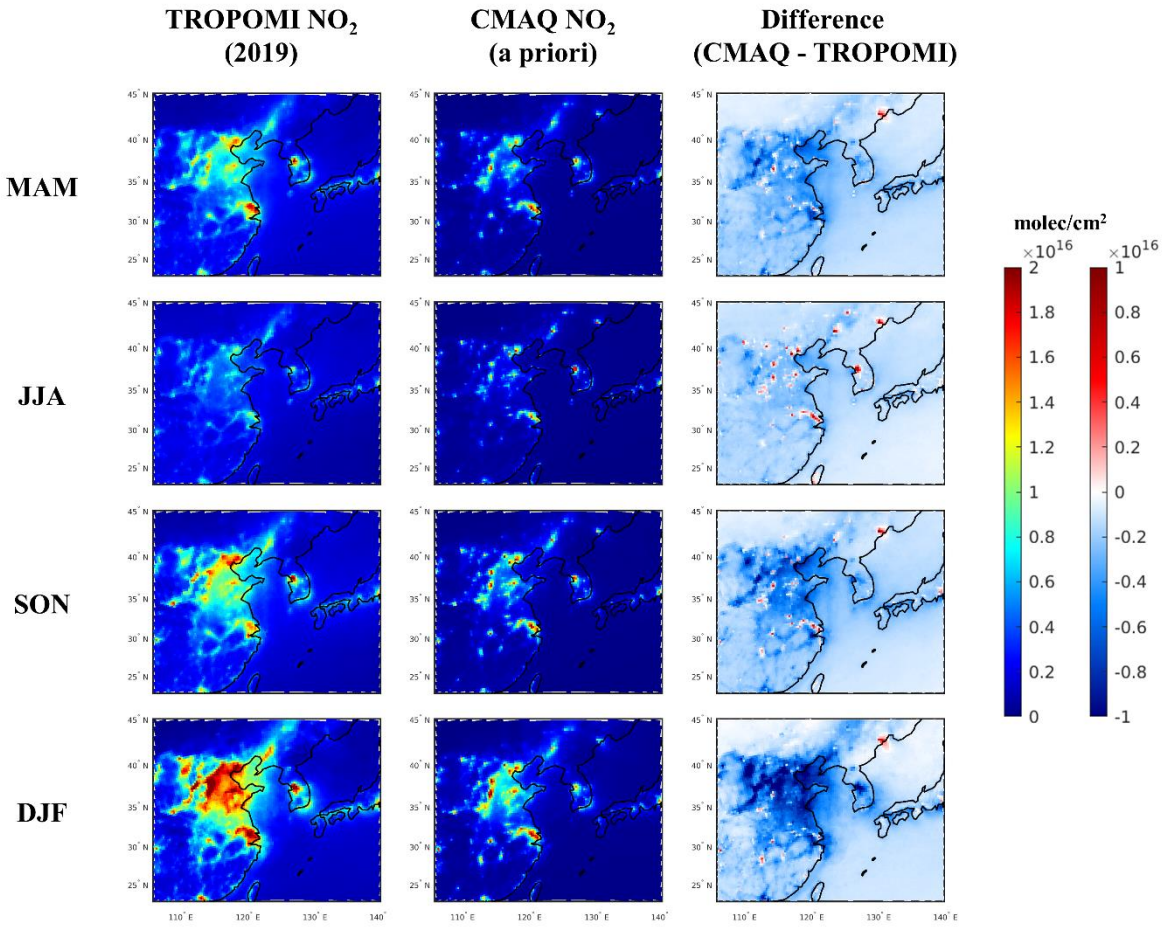

Figure S3. Spatial distributions of TROPOMI NO_2 columns (molec/cm^2) and CMAQ-simulated NO_2 columns before the NO_x emissions adjustment during the study period 2019. MAM: March, April, and May, JJA: June, July, and August, SON: September, October, and November, DJF: December, January, and February

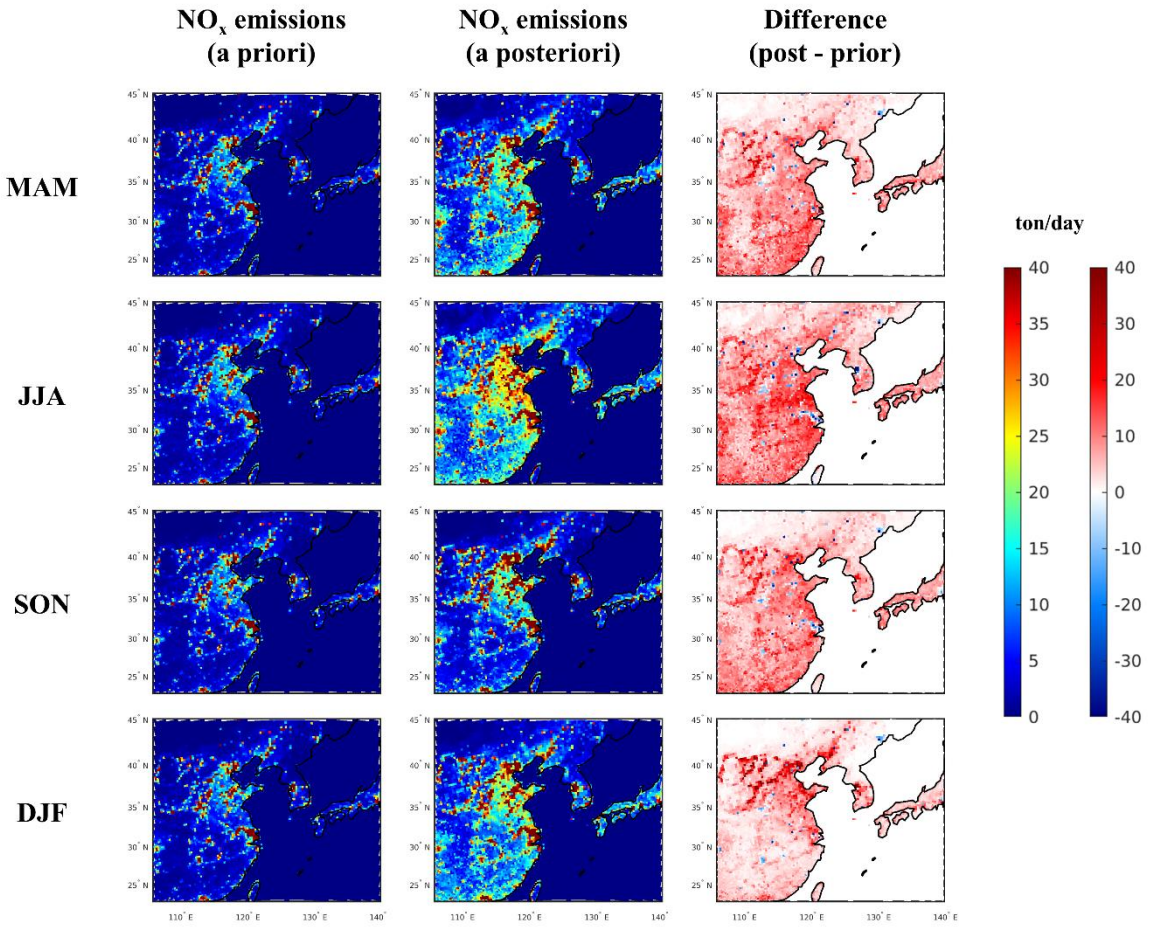

Figure S4. Spatial distributions of the bottom-up estimates of NO_x emissions (ton/day) before (a priori) and after (a posteriori) the NO_x emissions adjustment during the study period 2019.

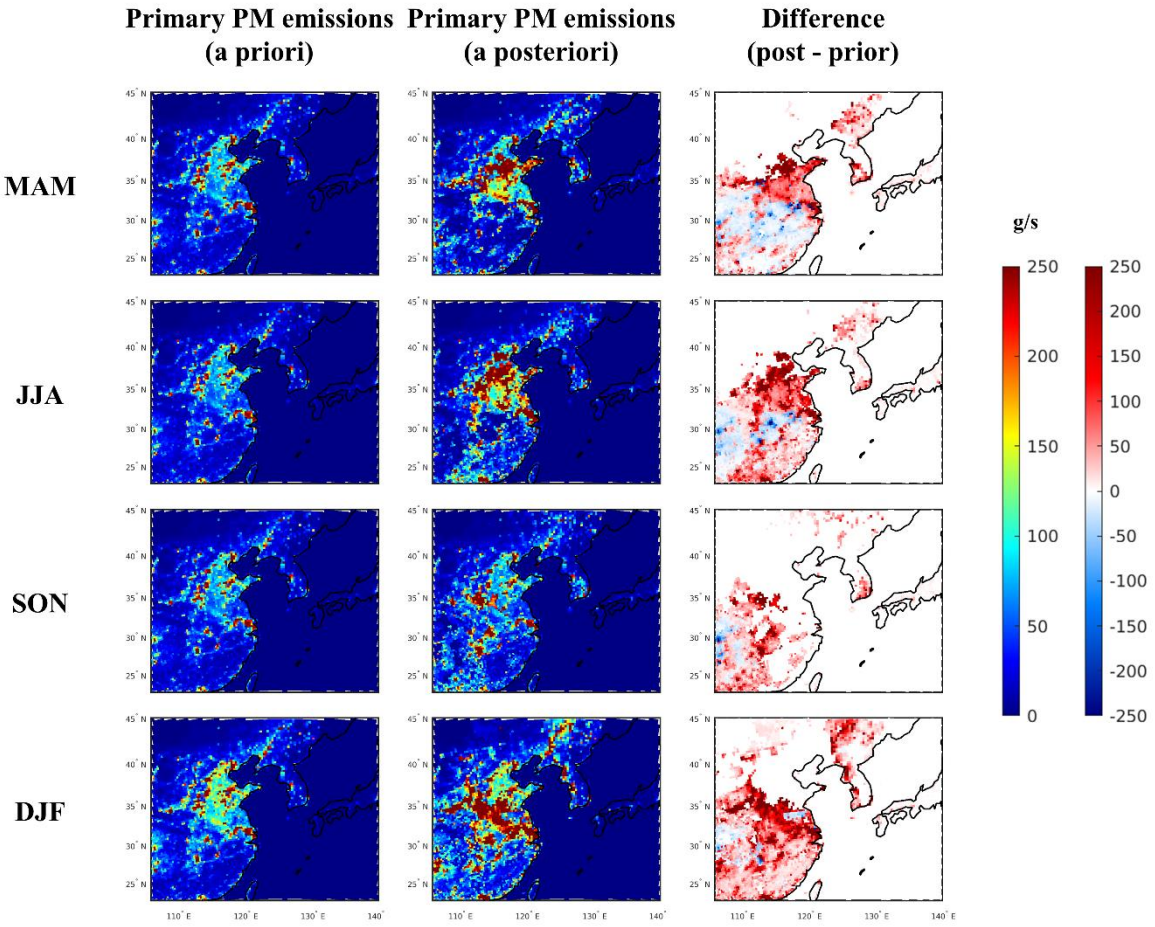

Figure S5. Spatial distributions of TROPOMI NO_2 columns, and CMAQ-simulated NO_2 columns before (a priori) and after (a posteriori) the NO_x emissions adjustment during the study period 2019. MAM: March, April, and May; JJA: June, July, and August; SON: September, October, and November; and DJF: December, January, and February.

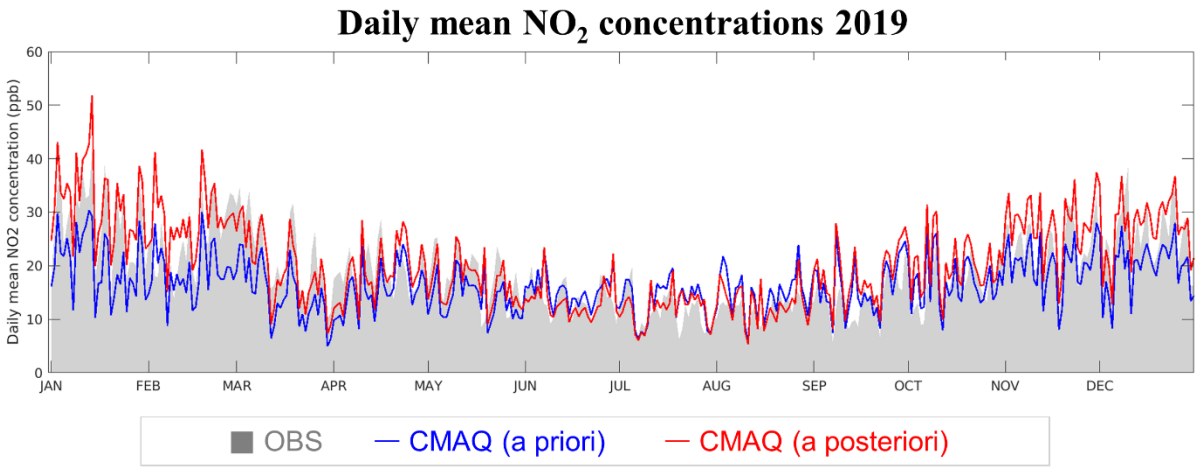

65

Figure S6. Comparisons of the time-series of the CMAQ-simulated daily mean surface NO_2 concentrations (ppb) before (a priori) and after (a posteriori) the NO_x emission adjustment, and the ground-based in-situ measurements in Korea (346 AirKorea sites) during the study period 2019. OBS: ground-based in-situ measurements.

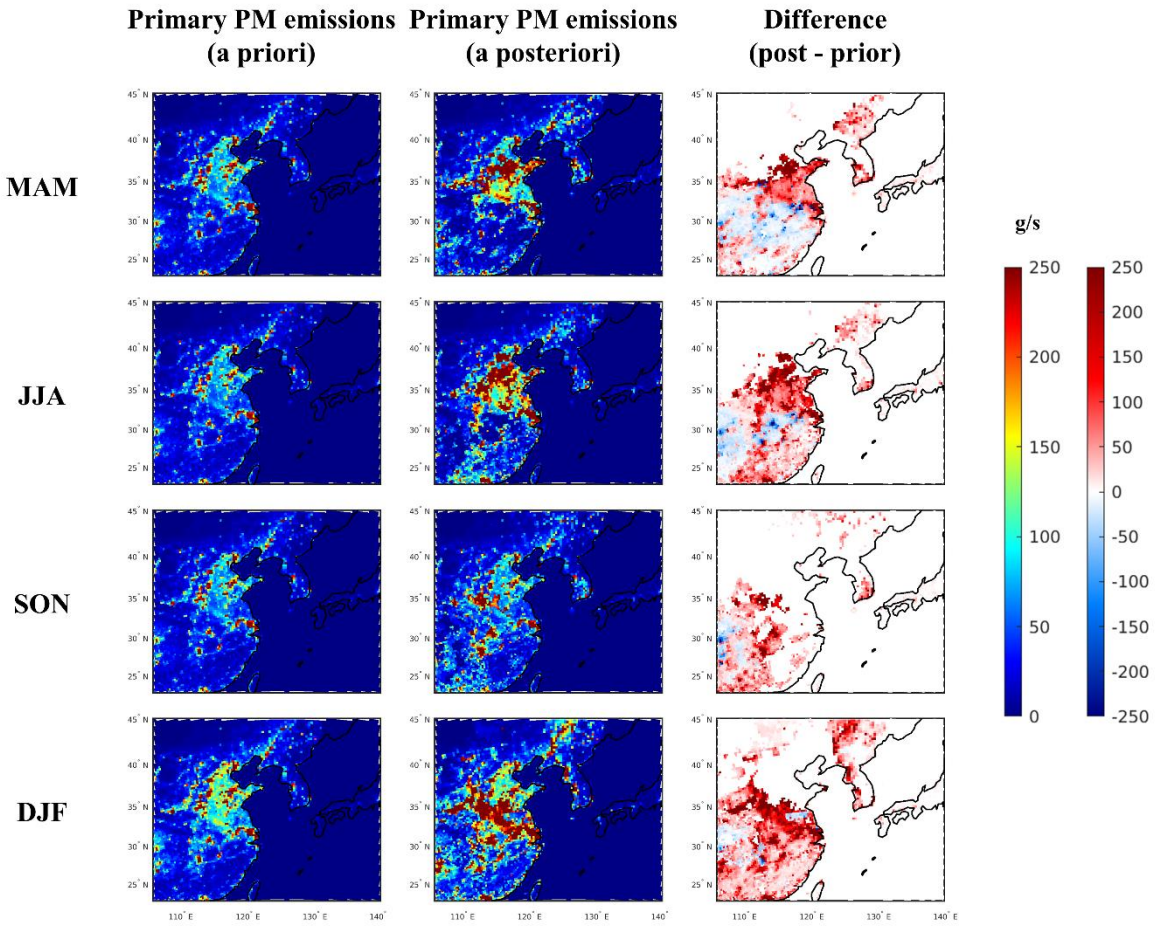

Figure S7. Spatial distributions of the bottom-up estimates of primary PM emissions (g/s) before (a priori) and after (a posteriori) the primary PM emissions adjustment (using the AHI AOD) during the study period 2019. The primary PM emissions here indicate the total amount of all primary PM species listed in Table S2.

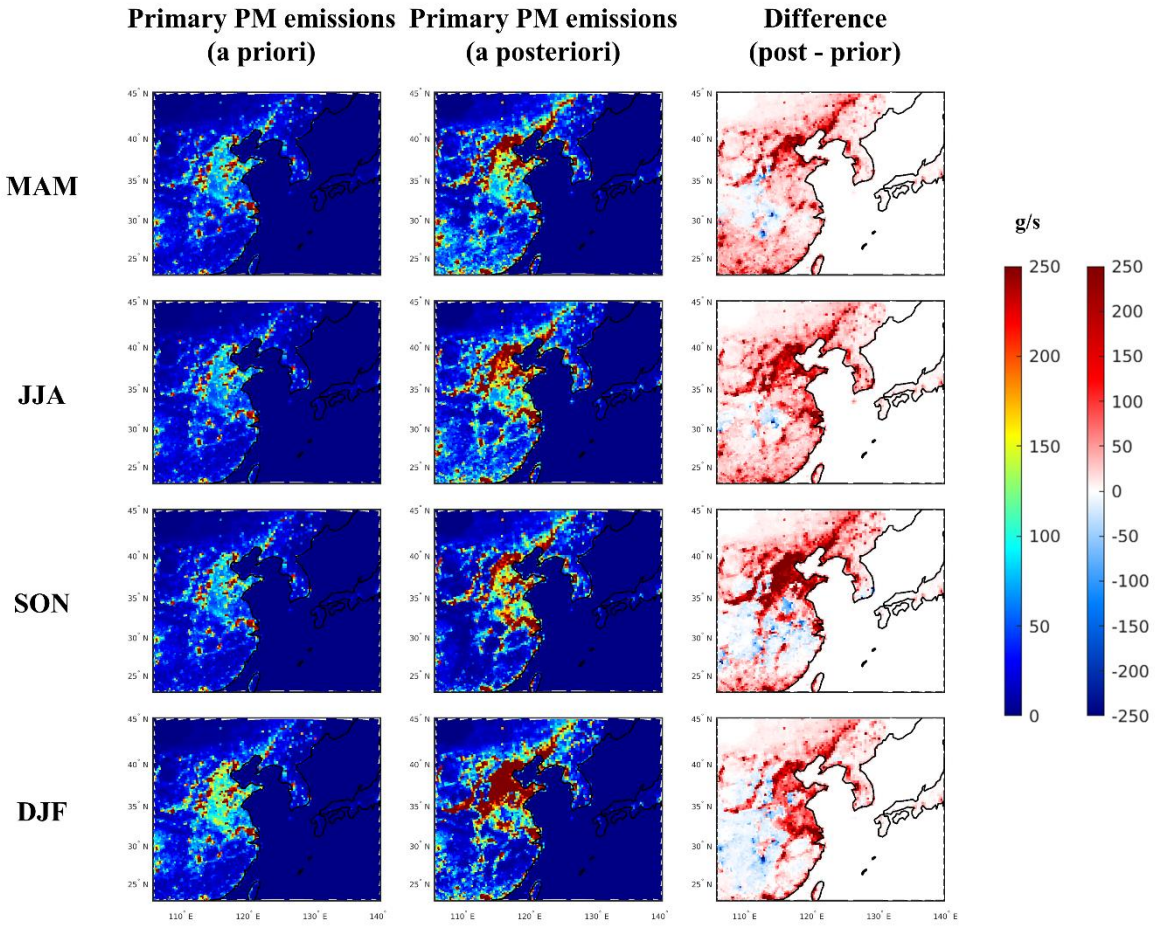

Figure S8. Spatial distributions of the bottom-up estimates of primary PM emissions (g/s) before (a priori) and after (a posteriori) the primary PM emissions adjustment (using GOCI-AHI fused AOD) during the study period 2019. The primary PM emissions here indicate the total amount of all primary PM species listed in Table S2.

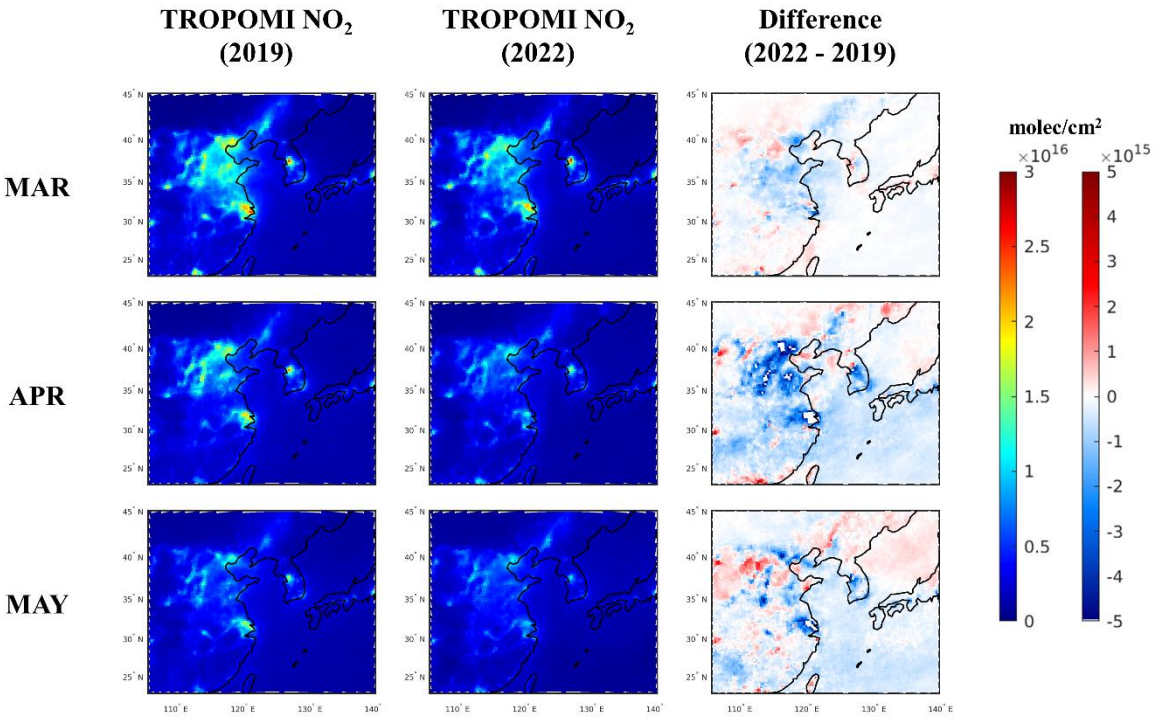

Figure S9. Spatial distributions of TROPOMI NO_2 columns (molec/cm^2) in March, April, and May 2019 and 2022.

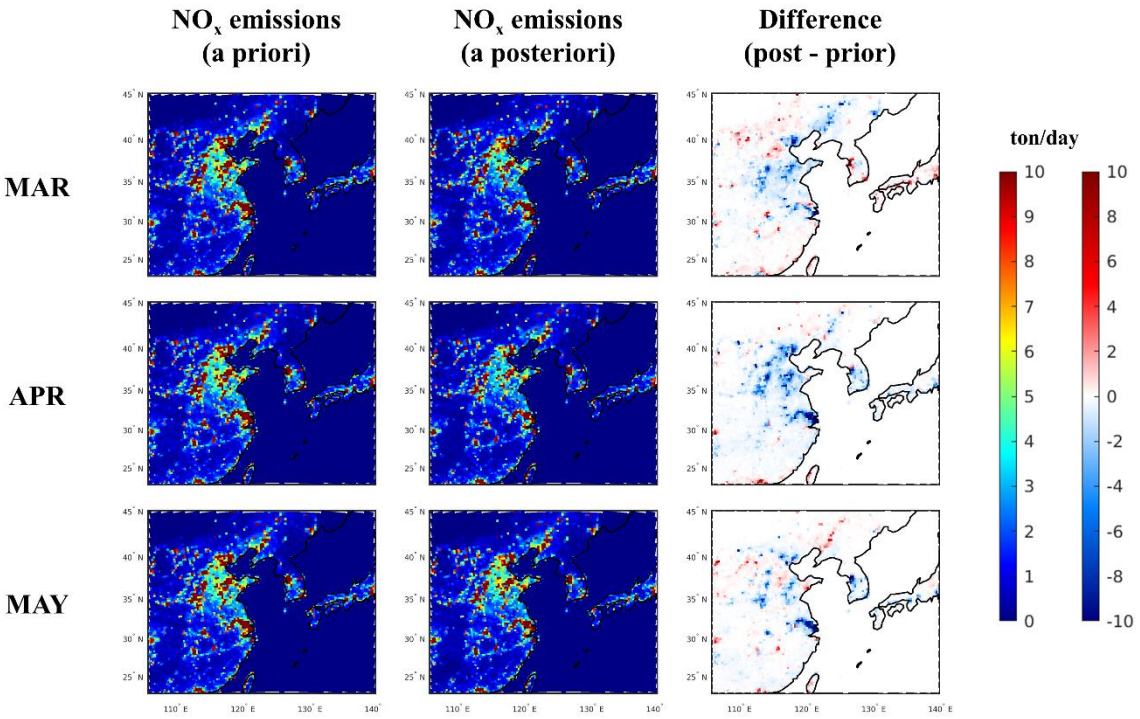

Figure S10. Spatial distributions of the bottom-up estimates of NO_x emissions (ton/day) before (a priori) and after (a posteriori) the NO_x emissions adjustment during the study period 2022.

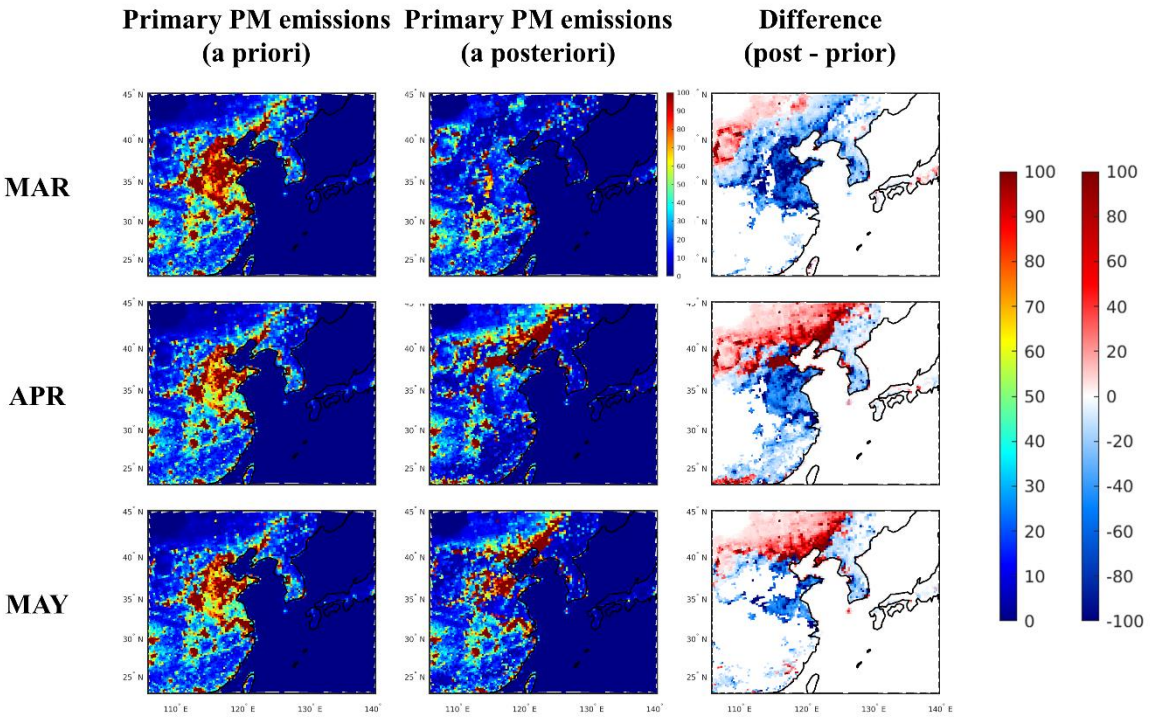

Figure S11. Spatial distributions of the bottom-up estimates of primary PM emissions (g/s) before (a priori) and after (a posteriori) the primary PM emissions adjustment (using GEMS-AMI-GOCI-2 fused AOD) during the study period 2022. The primary PM emissions here indicate the total amount of all primary PM species listed in Table S2.

References

Hatakeyama, S., Murano, K., Sakamaki, F., Mukai, H., Bandow, H., & Komazaki, Y. (2001). Transport of Atmospheric Pollutants from East Asia. *Water, Air, and Soil Pollution*, 130(1), 373–378. https://doi.org/10.1023/A:1013877000169

Ohara, T., Akimoto, H., Kurokawa, J., Horii, N., Yamaji, K., Yan, X., & Hayasaka, T. (2007). An Asian emission inventory of anthropogenic emission sources for the period 1980-2020. *Atmospheric Chemistry and Physics*, 7(16), 4419–4444. https://doi.org/10.5194/acp-7-4419-2007

Kumar, N., Chu, A., & Foster, A. (2007). An empirical relationship between $PM_{2.5}$ and aerosol optical depth in Delhi Metropolitan. *Atmospheric Environment*, 41(21), 4492–4503. https://doi.org/10.1016/j.atmosenv.2007.01.046

Tian, J. and Chen, D., 2010. Spectral, spatial, and temporal sensitivity of correlating MODIS aerosol optical depth with ground-based fine particulate matter (PM2.5) across southern Ontario. *Canadian Journal of Remote Sensing*, 36, 119-128. 10.5589/m10-033.

Remer, L. A., Mattoo, S., Levy, R. C., & Munchak, L. A. (2013). MODIS 3 km aerosol product: Algorithm and global perspective. *Atmospheric Measurement Techniques*, 6(7), 1829–1844. https://doi.org/10.5194/amt-6-1829-2013

Levy, R. C., Mattoo, S., Munchak, L. A., Remer, L. A., Sayer, A. M., Patadia, F., & Hsu, N. C. (2013). The Collection 6 MODIS aerosol products over land and ocean. *Atmospheric Measurement Techniques*, 6(11), 2989–3034. https://doi.org/10.5194/amt-6-2989-2013

Chan, P. K., Zhao, X.-P., & Heidinger, A. K. (2013). Long-Term Aerosol Climate Data Record Derived from Operational AVHRR Satellite Observations. *Dataset Papers in Geosciences*, 2013, e140791. https://doi.org/10.7167/2013/140791

Ahn, C., Torres, O., & Jethva, H. (2014). Assessment of OMI near-UV aerosol optical depth over land. *Journal of Geophysical Research: Atmospheres*, 119(5), 2457–2473. https://doi.org/10.1002/2013JD020188

Levy, R., Hsu, C., et al., 2015. MODIS Atmosphere L2 Aerosol Product. NASA MODIS Adaptive Processing System, Goddard Space Flight Center, USA: http://dx.doi.org/10.5067/MODIS/MOD04_L2.006

Garay, M. J., Witek, M. L., Kahn, R. A., Seidel, F. C., Limbacher, J. A., Bull, M. A., Diner, D. J., Hansen, E. G., Kalashnikova, O. V., Lee, H., Nastan, A. M., & Yu, Y. (2020). Introducing the 4.4 km spatial resolution Multi-Angle Imaging SpectroRadiometer (MISR) aerosol product. *Atmospheric Measurement Techniques*, 13(2), 593–628. https://doi.org/10.5194/amt-13-593-2020

Bellouin, N., Boucher, O., Haywood, J., & Reddy, M. S. (2005). Global estimate of aerosol direct radiative forcing from satellite measurements. *Nature*, 438(7071), 1138–1141. https://doi.org/10.1038/nature04348

Remer, L. A., Kleidman, R. G., Levy, R. C., Kaufman, Y. J., Tanré, D., Mattoo, S., Martins, J. V., Ichoku, C., Koren, I., Yu, H., & Holben, B. N. (2008). Global aerosol climatology from the MODIS satellite sensors. Journal of Geophysical Research: Atmospheres, 113(D14). https://doi.org/10.1029/2007JD009661

Munchak, L. A., Levy, R. C., Mattoo, S., Remer, L. A., Holben, B. N., Schafer, J. S., Hostetler, C. A., & Ferrare, R. A. (2013). MODIS 3 km aerosol product: Applications over land in an urban/suburban region. *Atmospheric Measurement Techniques*, 6(7), 1747–1759. https://doi.org/10.5194/amt-6-1747-2013

Filonchyk, M., Yan, H., Zhang, Z., Yang, S., Li, W., & Li, Y. (2019). Combined use of satellite and surface observations to study aerosol optical depth in different regions of China. Scientific Reports, 9(1), 6174. https://doi.org/10.1038/s41598-019-42466-6

Jung, J., Souri, A. H., Wong, D. C., Lee, S., Jeon, W., Kim, J., & Choi, Y. (2019). The Impact of the Direct Effect of Aerosols on Meteorology and Air Quality Using Aerosol Optical Depth Assimilation During the KORUS-AQ Campaign. *Journal of Geophysical Research: Atmospheres*, 124(14), 8303–8319. https://doi.org/10.1029/2019JD030641

Jung, J., Choi, Y., Wong, D. C., Nelson, D., & Lee, S. (2021). Role of Sea Fog Over the Yellow Sea on Air Quality With the Direct Effect of Aerosols. *Journal of Geophysical Research: Atmospheres*, 126(5), e2020JD033498. https://doi.org/10.1029/2020JD033498

Lee, K., Kim, M., Choi, M., Kim, K., Choi, Y., Jeong, J., Moon, K-J., & Lee, S. (2022). Fast and operational gap filling in satellite-derived aerosol optical depths using statistical techniques. *J. Appl. Rem. Sens*, 16(4). https://doi.org/10.1117/1.JRS.16.044507

Byun, D., & Schere, K. L. (2006). Review of the Governing Equations, Computational Algorithms, and Other Components of the Models-3 Community Multiscale Air Quality (CMAQ) Modeling System. *Applied Mechanics Reviews*, 59(2), 51–77. https://doi.org/10.1115/1.2128636

Wang, J., Xu, X., Henze, D. K., Zeng, J., Ji, Q., Tsay, S.-C., & Huang, J. (2012). Top-down estimate of dust emissions through integration of MODIS and MISR aerosol retrievals with the GEOS-Chem adjoint model. Geophysical Research Letters, 39(8). https://doi.org/10.1029/2012GL051136

Ku, B., & Park, R. J. (2013). Comparative inverse analysis of satellite (MODIS) and ground (PM10) observations to estimate dust emissions in East Asia. *Asia-Pacific Journal of Atmospheric Sciences*, 49(1), 3–17. https://doi.org/10.1007/s13143-013-0002-5

Koo, Y.-S., Choi, D.-R., Kwon, H.-Y., Jang, Y.-K., & Han, J.-S. (2015). Improvement of PM10 prediction in East Asia using inverse modeling. *Atmospheric Environment*, 106, 318–328. https://doi.org/10.1016/j.atmosenv.2015.02.004

Pang, J., Liu, Z., Wang, X., Bresch, J., Ban, J., Chen, D., & Kim, J. (2018). Assimilating AOD retrievals from GOCI and VIIRS to forecast surface PM2.5 episodes over Eastern China. *Atmospheric Environment*, 179, 288–304. https://doi.org/10.1016/j.atmosenv.2018.02.011

Xia, X., Min, J., Shen, F., Wang, Y., & Yang, C. (2019). Aerosol Data Assimilation Using Data from Fengyun-3A and MODIS: Application to a Dust Storm over East Asia in 2011. *Advances in Atmospheric Sciences*, 36(1), 1–14. https://doi.org/10.1007/s00376-018-8075-9

Wang, Y., Wang, J., Xu, X., Henze, D. K., Qu, Z., & Yang, K. (2020). Inverse modeling of SO2 and NOx emissions over China using multisensor satellite data – Part 1: Formulation and sensitivity analysis. *Atmospheric Chemistry and Physics*, 20(11), 6631–6650. https://doi.org/10.5194/acp-20-6631-2020

Li, N., Tang, K., Wang, Y., Wang, J., Feng, W., Zhang, H., Liao, H., Hu, J., Long, X., Shi, C., & Su, X. (2021). Is the efficacy of satellite-based inversion of SO2 emission model dependent? *Environmental Research Letters*, 16(3), 035018. https://doi.org/10.1088/1748-9326/abe829

Lee, S., Song, C. H., Han, K. M., Henze, D. K., Lee, K., Yu, J., Woo, J.-H., Jung, J., Choi, Y., Saide, P. E., & Carmichael, G. R. (2022). Impacts of uncertainties in emissions on aerosol data assimilation and short-term PM2.5 predictions over Northeast Asia. Atmospheric Environment, 271, 118921. https://doi.org/10.1016/j.atmosenv.2021.118921

Vijayaraghavan, K., Snell, H. E., & Seigneur, C. (2008). Practical Aspects of Using Satellite Data in Air Quality Modeling. *Environmental Science & Technology*, 42(22), 8187–8192. https://doi.org/10.1021/es7031339

Jeon, W., Choi, Y., Percell, P., Souri, A. H., Song, C.-K., Kim, S.-T., & Kim, J. (2016). Computationally efficient air quality forecasting tool: Implementation of STOPS v1.5 model into CMAQ v5.0.2 for a prediction of Asian dust. *Geoscientific Model Development*, 9(10), 3671–3684. https://doi.org/10.5194/gmd-9-3671-2016

Lee, S., Song, C. H., Park, R. S., Park, M. E., Han, K. M., Kim, J., et al. (2016). GIST-PM-Asia v1: Development of a numerical system to improve particulate matter forecasts in South Korea using geostationary satellite-retrieved aerosol optical data over Northeast Asia. *Geoscientific Model Development*, 9(1), 17–39. https://doi.org/10.5194/gmd-9-17-2016

Yumimoto, K., Nagao, T. m., Kikuchi, M., Sekiyama, T. t, Murakami, H., Tanaka, T. y., Ogi, A., Irie, H., Khatri, P., Okumura, H., Arai, K., Morino, I., Uchino, O., & Maki, T. (2016). Aerosol data assimilation using data from Himawari-8, a next-generation geostationary meteorological satellite. *Geophysical Research Letters*, 43(11), 5886–5894. https://doi.org/10.1002/2016GL069298

Jin, J., Segers, A., Heemink, A., Yoshida, M., Han, W., & Lin, H.-X. (2019). Dust Emission Inversion Using Himawari-8 AODs Over East Asia: An Extreme Dust Event in May 2017. *Journal of Advances in Modeling Earth Systems*, 11(2), 446–467. https://doi.org/10.1029/2018MS001491

Choi, W. J., and Coauthors, 2018: Introducing the Geostationary Environment Monitoring Spectrometer. J. Appl. Remote Sens., 13, 044005, https://doi.org/10.1117/1.JRS.12.044005

Kim, J., Choi, M., Kim, M., Lim, H., Lee, S., Moon, K. J., Choi, W. J., Yoon, J. M., Kim, S.-K., Ko, D. H., Lee, S. H., Park, Y., & Chung, C.-Y. (2018). Monitoring Atmospheric Composition by Geo-Kompsat-2: Goci-2, Ami and Gems. IGARSS 2018 - 2018 IEEE International Geoscience and Remote Sensing Symposium, 7750–7752. https://doi.org/10.1109/IGARSS.2018.8518713

Kim, J., Jeong, U., Ahn, M.-H., Kim, J. H., Park, R. J., Lee, H., Song, C. H., Choi, Y.-S., Lee, K.-H., Yoo, J.-M., Jeong, M.-J., Park, S. K., Lee, K.-M., Song, C.-K., Kim, S.-W., Kim, Y. J., Kim, S.-W., Kim, M., Go, S., … Choi, Y. (2020a). New Era of Air Quality Monitoring from Space: Geostationary Environment Monitoring Spectrometer (GEMS). *Bulletin of the American Meteorological Society*, 101(1), E1–E22. https://doi.org/10.1175/BAMS-D-18-0013.1

Zoogman, P., and Coauthors, 2011: Ozone air quality measurement requirements for a geostationary satellite mission. *Atmos. Environ.*, 45, 7143–7150, https://doi.org/10.1016/j.atmosenv.2011.05.058

Ingmann, P., B. Veihelmann, J. Langen, D. Lamarre, H. Stark, and G. B. Courrèges-Lacoste, 2012: Requirements for the GMES atmosphere service and ESA's implementation concept: Sentinels-4/-5 and -5p. *Remote Sens. Environ.*, 120, 58–69, https://doi.org/10.1016/j.rse.2012.01.023

Zou, B., Liu, N., Wang, W., Feng, H., Liu, X., & Lin, Y. (2020). An Effective and Efficient Enhanced Fixed Rank Smoothing Method for the Spatiotemporal Fusion of Multiple-Satellite Aerosol Optical Depth Products. *Remote Sensing*, 12(7), Article 7. https://doi.org/10.3390/rs12071102

Choi, M., Lim, H., Kim, J., Lee, S., Eck, T. F., Holben, B. N., Garay, M. J., Hyer, E. J., Saide, P. E., & Liu, H. (2019). Validation, comparison, and integration of GOCI, AHI, MODIS, MISR, and VIIRS aerosol optical depth over East Asia during the 2016 KORUS-AQ campaign. *Atmospheric Measurement Techniques*, 12(8), 4619–4641. https://doi.org/10.5194/amt-12-4619-2019

Go, S., Kim, J., Park, S. S., Kim, M., Lim, H., Kim, J.-Y., Lee, D.-W., & Im, J. (2020). Synergistic Use of Hyperspectral UV-Visible OMI and Broadband Meteorological Imager MODIS Data for a Merged Aerosol Product. *Remote Sensing*, *12*(23), Article 23. https://doi.org/10.3390/rs12233987

Lim, H., Go, S., Kim, J., Choi, M., Lee, S., Song, C.-K., & Kasai, Y. (2021). Integration of GOCI and AHI Yonsei aerosol optical depth products during the 2016 KORUS-AQ and 2018 EMeRGe campaigns, Atmospheric Measurement Techniques, 14, 4575-4592

Holben, B. N., Eck, T. F., Slutsker, I., Tanr´e, D., Buis, J. P., Setzer, A., Vermote, E., Reagan, J. A., Kaufmann, Y. J., Nakajima, T., Lavenu, F., Jankowiak, I., and Smirnov, A. (1998). AERONET: A federated instrument network and data archive for aerosol characterisation, *Remote Sens. Environ.*, 66, 1–16

Dyer, O. (2022). Covid-19: Lockdowns spread in China as omicron tests "zero covid" strategy. *BMJ*, 376, o859. https://doi.org/10.1136/bmj.o859

Woo, J.-H., Kim, Y., Kim, H.-K., Choi, K.-C., Eum, J.-H., Lee, J.-B., Lim, J.-H., Kim, J., & Seong, M. (2020). Development of the CREATE Inventory in Support of Integrated Climate and Air Quality Modeling for Asia. *Sustainability*, 12(19), 7930. https://doi.org/10.3390/su12197930

Jang, Y., Lee, Y., Kim, J., Kim, Y., Woo, J.-H. (2019). Improvement China Point Source for Improving Bottom-Up Emission Inventory. *Asia Pac. J. Atmos. Sci.*, 56, 107–118

Yeo, S.Y., Lee, H.K., Choi, S.W, Seol, S.H., Jin, H.A., Yoo, C., Lim, J.Y., Kim, J.S. (2019). Analysis of the national air pollutant emission inventory (CAPSS 2015) and the major cause of change in Republic of Korea. *Asian J. Atmos. Environ.* 13 (3), 212–231. https://doi.org/10.5572/ajae.2019.13.3.212

Toon, O. B., et al. (2016), Planning, implementation and scientific goals of the Studies of Emissions and Atmospheric Composition, Clouds and Climate Coupling by Regional Surveys (SEAC4RS) field mission, *J. Geophys. Res. Atmos.*, 121, 4967–5009, doi:10.1002/2015JD024297

Guenther, A. B., Jiang, X., Heald, C. L., Sakulyanontvittaya, T., Duhl, T., Emmons, L. K., & Wang, X. (2012). The Model of Emissions of Gases and Aerosols from Nature version 2.1 (MEGAN2.1): An extended and updated framework for

modeling biogenic emissions. *Geoscientific Model Development*, 5(6), 1471–1492. https://doi.org/10.5194/gmd-5-1471-2012

Guenther, A.B., Karl, T., Harley, P., Wiedinmyer, C., Palmer, P. I., & Geron, C. (2006). Estimates of global terrestrial isoprene emissions using MEGAN (Model of Emissions of Gases and Aerosols from Nature). *Atmospheric Chemistry and Physics*, 6(11), 3181–3210. https://doi.org/10.5194/acp-6-3181-2006

Guenther, A., Jiang, X., Shah, T., Huang, L., Kemball-Cook, S., & Yarwood, G. (2020). Model of Emissions of Gases and Aerosol from Nature Version 3 (MEGAN3) for Estimating Biogenic Emissions. In C. Mensink, W. Gong, & A. Hakami (Eds.), Air Pollution Modeling and its Application XXVI (pp. 187–192). Springer International Publishing. https://doi.org/10.1007/978-3-030-22055-6_29

Yuan, H., Dai, Y., Xiao, Z., Ji, D., & Shangguan, W. (2011). Reprocessing the MODIS Leaf Area Index products for land surface and climate modelling. *Remote Sensing of Environment*, 115(5), 1171–1187. https://doi.org/10.1016/j.rse.2011.01.001

Jiang, Z., Vargas, M., & Csiszar, I. (2016). New oprational real-time daily rolling weekly Green Vegetation fraction product derived from suomi NPP VIIRS reflectance data. 2016 IEEE International Geoscience and Remote Sensing Symposium (IGARSS), 3524–3527. https://doi.org/10.1109/IGARSS.2016.7729911

Skamarock, W. C., Klemp, J. B., Dudhia, J., Gill, D. O., Barker, D., Duda, M. G., … Powers, J. G. (2008). A Description of the Advanced Research WRF Version 3 (No. NCAR/TN-475+STR). University Corporation for Atmospheric Research. https://doi.org/10.5065/D68S4MVH

Pouyaei, A., Choi, Y., Jung, J., Sadeghi, B., & Song, C. H. (2020). Concentration Trajectory Route of Air pollution with an Integrated Lagrangian model (C-TRAIL Model v1.0) derived from the Community Multiscale Air Quality Model (CMAQ Model v5.2). *Geoscientific Model Development*, 13(8), 3489–3505. https://doi.org/10.5194/gmd-13-3489-2020

Pouyaei, A., Sadeghi, B., Choi, Y., Jung, J., Souri, A. H., Zhao, C., & Song, C. H. (2021). Development and Implementation of a Physics-Based Convective Mixing Scheme in the Community Multiscale Air Quality Modeling Framework. *Journal of Advances in Modeling Earth Systems*, 13(6), e2021MS002475. https://doi.org/10.1029/2021MS002475

Park, J., Jung, J., Choi, Y., Mousavinezhad, S., & Pouyaei, A. (2022). The sensitivities of ozone and PM2.5 concentrations to the satellite-derived leaf area index over East Asia and its neighboring seas in the WRF-CMAQ modeling system. *Environmental Pollution*, 306, 119419. https://doi.org/10.1016/j.envpol.2022.119419

Veefkind, J. P., Aben, I., McMullan, K., Förster, H., de Vries, J., Otter, G., Claas, J., Eskes, H. J., de Haan, J. F., Kleipool, Q., van Weele, M., Hasekamp, O., Hoogeveen, R., Landgraf, J., Snel, R., Tol, P., Ingmann, P., Voors, R., Kruizinga, B., … Levelt, P. F. (2012). TROPOMI on the ESA Sentinel-5 Precursor: A GMES mission for global observations of the atmospheric composition for climate, air quality and ozone layer applications. *Remote Sensing of Environment*, 120, 70–83. https://doi.org/10.1016/j.rse.2011.09.02

Okuyama, A., Andou, A., Date, K., Hoasaka, K., Mori, N., Murata, H., Tabata, T., Takahashi, M., Yoshino, R., & Bessho, K. (2015). Preliminary validation of Himawari-8/AHI navigation and calibration. *Earth Observing Systems*, 9607, 663–672. https://doi.org/10.1117/12.2188978

Bessho, K., Date, K., Hayashi, M., Ikeda, A., Imai, T., Inoue, H., Kumagai, Y., Miyakawa, T., Murata, H., Ohno, T., Okuyama, A., Oyama, R., Sasaki, Y., Shimazu, Y., Shimoji, K., Sumida, Y., Suzuki, M., Taniguchi, H., Tsuchiyama, H., … Yoshida, R. (2016). An Introduction to Himawari-8/9—Japan's New-Generation Geostationary Meteorological Satellites. *Journal of the Meteorological Society of Japan*. Ser. II, 94(2), 151–183. https://doi.org/10.2151/jmsj.2016-009

Pitchford, M., Maim, W., Schichtel, B., Kumar, N., Lowenthal, D., & Hand, J. (2007). Revised algorithm for estimating light extinction from IMPROVE particle speciation data. *Journal of the Air & Waste Management Association* 57(11), 1326–1336. https://doi.org/10.3155/1047-3289.57.11.1326

ÅngstrÖm, A. (1961). Techniques of Determining the Turbidity of the Atmosphere. *Tellus*, 13(2), 214–223. https://doi.org/10.3402/tellusa.v13i2.9493

Choi, M., Kim, J., Lee, J., Kim, M., Park, Y.-J., Jeong, U., Kim, W., Hong, H., Holben, B., Eck, T. F., Song, C. H., Lim, J.-H., & Song, C.-K. (2016). GOCI Yonsei Aerosol Retrieval (YAER) algorithm and validation during the DRAGON-NE Asia 2012 campaign. *Atmospheric Measurement Techniques*, 9(3), 1377–1398. https://doi.org/10.5194/amt-9-1377-2016

Choi, M., Kim, J., Lee, J., Kim, M., Park, Y.-J., Holben, B., Eck, T. F., Li, Z., & Song, C. H. (2018). GOCI Yonsei aerosol retrieval version 2 products: An improved algorithm and error analysis with uncertainty estimation from 5-year validation over East Asia. *Atmospheric Measurement Techniques*, 11(1), 385–408. https://doi.org/10.5194/amt-11-385-2018

Lim, H., Choi, M., Kim, J., Kasai, Y., & Chan, P. W. (2018). AHI/Himawari-8 Yonsei Aerosol Retrieval (YAER): Algorithm, Validation and Merged Products. *Remote Sensing*, 10(5), 699. https://doi.org/10.3390/rs10050699

Chung, S.-R., Ahn, M.-H., Han, K.-S., Lee, K.-T., & Shin, D.-B. (2020). Meteorological Products of Geo-KOMPSAT 2A (GK2A) Satellite. *Asia-Pacific Journal of Atmospheric Sciences*, 56(2), 185–185. https://doi.org/10.1007/s13143-020-00199-x

Kim, D., Gu, M., Oh, T.-H., Kim, E.-K., & Yang, H.-J. (2021). Introduction of the Advanced Meteorological Imager of Geo-Kompsat-2a: In-Orbit Tests and Performance Validation. *Remote Sensing*, 13(7), Article 7. https://doi.org/10.3390/rs13071303

Kim, M., Kim, J., Lim, H., & Chan, P. W. (2020b). The implementation of Yonsei Aerosol Retrieval (YAER) Algorithm to GK-2A/AMI and FY-4A/AGRI. American Geophysical Union, Fall Meeting 2020, A141-0007.

Rodgers, C.D. (2000). Inverse Methods for Atmospheric Sounding: Theory and Practice, Series on Atmospheric, Oceanic and Planetary Physics. WORLD SCIENTIFIC. https://doi.org/10.1142/3171

Souri, A. H., Nowlan, C. R., González Abad, G., Zhu, L., Blake, D. R., Fried, A., Weinheimer, A. J., Wisthaler, A., Woo, J.-H., Zhang, Q., Chan Miller, C. E., Liu, X., & Chance, K. (2020). An inversion of NO_x and non-methane volatile organic compound (NMVOC) emissions using satellite observations during the KORUS-AQ campaign and implications for surface ozone over East Asia. *Atmospheric Chemistry and Physics*, 20(16), 9837–9854. https://doi.org/10.5194/acp-20-9837-2020

Jung, J., Choi, Y., Souri, A. H., Mousavinezhad, S., Sayeed, A., & Lee, K. (2022). The Impact of Springtime-Transported Air Pollutants on Local Air Quality With Satellite-Constrained NO_x Emission Adjustments Over East Asia. *Journal of Geophysical Research: Atmospheres*, 127(5), e2021JD035251. https://doi.org/10.1029/2021JD035251

Napelenok, S. L., Cohan, D. S., Hu, Y., & Russell, A. G. (2006). Decoupled direct 3D sensitivity analysis for particulate matter (DDM-3D/PM). *Atmospheric Environment*, 40(32), 6112–6121. https://doi.org/10.1016/j.atmosenv.2006.05.039

Zhang, W., Xu, H., & Zheng, F. (2018). Aerosol Optical Depth Retrieval over East Asia Using Himawari-8/AHI Data. *Remote Sensing*, 10(1), 137. https://doi.org/10.3390/rs10010137

Martin, R. V., Jacob, D. J., Chance, K., Kurosu, T. P., Palmer, P. I., & Evans, M. J. (2003). Global inventory of nitrogen oxide emissions constrained by space-based observations of NO2 columns. *Journal of Geophysical Research: Atmospheres*, 108(D17). https://doi.org/10.1029/2003JD003453

Cooper, M., Martin, R. V., Padmanabhan, A., & Henze, D. K. (2017). Comparing mass balance and adjoint methods for inverse modeling of nitrogen dioxide columns for global nitrogen oxide emissions. *Journal of Geophysical Research: Atmospheres*, 122(8), 4718–4734. https://doi.org/10.1002/2016JD025985

Mousavinezhad, S., Choi, Y., Pouyaei, A., Ghahremanloo, M., & Nelson, D. L. (2021). A comprehensive investigation of surface ozone pollution in China, 2015–2019: Separating the contributions from meteorology and precursor emissions. Atmospheric Research, 257, 105599. https://doi.org/10.1016/j.atmosres.2021.105599

Chen, L., Fei, Y., Wang, R., Fang, P., Han, J., & Zha, Y. (2021). Retrieval of High Temporal Resolution Aerosol Optical Depth Using the GOCI Remote Sensing Data. *Remote Sensing*, 13(12), 2376. https://doi.org/10.3390/rs13122376

Caporale, G. M., Carmona-González, N., & Gil-Alana, L. A. (2022). Atmospheric Pollution in Chinese Cities: Trends and Persistence (SSRN Scholarly Paper No. 4309213). https://doi.org/10.2139/ssrn.4309213

Chen, L., Mao, F., Hong, J., Zang, L., Chen, J., Zhang, Y., Gan, Y., Gong, W., & Xu, H. (2022). Improving PM2.5 predictions during COVID-19 lockdown by assimilating multi-source observations and adjusting emissions. *Environmental Pollution*, 297, 118783. https://doi.org/10.1016/j.envpol.2021.118783

Li, K., Ni, R., Jiang, T., Tian, Y., Zhang, X., Li, C., & Xie, C. (2022). The regional impact of the COVID-19 lockdown on the air quality in Ji'nan, China. Scientific Reports, 12(1), Article 1. https://doi.org/10.1038/s41598-022-16105-6

Carmichael, G.R., Streets, D.G., Calori, G., Amann, M., Jacobson, M.Z., Hansen, J., & Ueda, H. (2002). Changing trends in sulfur emissions in Asia: Implications for acid deposition. *Environ. Sci. Technol.*, 36, 4707-4713, doi:10.1021/es011509c.